Formation of super-Earths via pebble accretion onto planetesimals

Daniel Mikkola

Lund Observatory
Lund University

2015-EXA93

Degree project of 15 higher education credits
May 2015

Supervisor: Anders Johansen

Lund Observatory
Box 43
SE-221 00 Lund
Sweden

Abstract

Data from NASA's Kepler space telescope, which searches for exoplanets via the transit method, produced 1108 new planetary candidates in 2013 with a total of 91% being smaller than Neptune in size. These were mostly super-Earths, terrestial planets between Earth and Neptune in size, with orbits around 10 days.

In order for any theory of planet formation to be valid it must be able to account for the existence of these super-Earths. Current models put the transition from planetesimal to planet to be the result of planetesimal collisions. In only the past few years the theory of pebble accretion onto planetesimals has emerged. It centers around the idea that the accretion of pebbles onto planetesimals in the protoplanetary disk is a large part of planet formation, able to rapidly speed the process up.

In this thesis we investigate whether the pebble accretion theory can account for the super-Earths in Kepler's data. This is done using a statistical code called PAOPAP. We simulate the accretion of mm-cm sized pebbles onto already existing planetesimals and investigate what effect different sized annuli and the amount of pebbles has on the final mass of the planets produced in the code. We find that while wider annuli make no discernible pattern in the final mass of the planets, increasing the amount of mass in pebbles for a 0.2 AU annulus allows us to create planets with masses up to $\sim$8 M_{E} or $\sim$2 R_{E}. The reason the annulus width does not determine mass is because the planets become isolated at a certain point, having accreted all nearby pebbles, giving them an isolation mass. We also vary the size of the pebbles being accreted to show that larger pebbles only brings about a faster growth process but with the same final mass in a simulation. Lastly we show a selection of the largest planetesimals in each simulation to give a demonstration of oligarchic growth of planets over time. In the end, we are able to show that the large population of super-Earths found by the Kepler satellite can be explained by the theory of pebble accretion.

Acknowledgements

I would like to express my gratitude to my supervisor, Anders Johansen, for his continued advice and support through the writing of this thesis. I especially appreciated our conversations on Tolkien and Lovecraft which showed me that there is room for entertainment even during the most stressful of hours.

Populärvetenskaplig beskrivning

Sedan urminnes tider har man vetat om att det finns ljusa kroppar på himlen som rör sig ovanligt fort. Grekerna döpte dessa till vandrare, ett ord som på grekiska uttalas väldigt likt planet. Planeterna har studerats i århundraden och bara de senaste två decennierna har vi ökat från våra egna åtta planeter till flera tusen nya planeter kallade *exoplaneter*, planeter runt andra stjärnor än våran egen.

En naturlig fråga som följer utav detta är skapelsen av planeter. På 1700-talet argumenterade personer som Immanuel Kant och Pierre Simon de Laplace för en planetformationsteori. Man noterade då att de sex planeter man kände till rörde sig i nästan perfekt cirkulära omloppsbanor samt rörde sig i nästan exakt samma plan. Argumentet var då att planeterna hade formats i en tillplattad skiva runt solen. Idén om en skiva runt solen har levt vidare sedan dess. På 60-talet kom en sovjetisk astronom vid namnet Viktor Safronov fram med sin nya hypotes, planetesimal-hypotesen. I den berättar Safronov om hur planeter skapats av en lång serie händelser i skivan, ursprungligen som mikroskopiska dammkorn som krockar och klumpar ihop sig. De blir större tills de bildar planetesimaler. Dessa är kroppar i storleksordningen några meter till 100 km. Planetesimalerna fortsätter kollidera till nästa storleksordning, protoplaneter, och blir i slutändan planeter.

Under de senaste åren har en ny teori utvecklats som kallas för *Pebble Accretion*, vilket betyder ungefär ansamling av gruskorn. I ledning av Anders Johansen utvecklades teorin vid Lunds Universitet och den motsäger sig inte Safronovs hypotes utan istället säger att under steget från planetesimaler till planeter borde det också finnas gruskorn i mm-cm storlek i skivan som ansamlas på planetesimalen. Pebble accretion har senare visat sig kunna snabba upp planetformation med så mycket som en faktor tusen, en stor ökning. Detta är väldigt eftertraktat då man vill skapa en planet innan skivans material försvinner på grund av andra orsaker vilket tar ungefär 10 miljoner år.

Pebble accretion utvecklas ännu och med flera utmaningar kan den visa sig lovande. NASAs rymdteleskop Kepler, som letar efter exoplaneter, presenterade 2013 resultat på 1108 nya planetkandidater, planeter som upptäckts en gång och man inte är säker på om det faktiskt är planeter. Mest märkvärdigt var att utav de 1108 planeterna var så många som 91% mindre än Neptunus och nästan alla var större än Jorden. Denna storleksordning kallas super-Earths, planeter som förmodligen är jordlika, men med större massa än Jorden.

Detta utgör ett perfekt test för pebble accretion. Om teorin ska hålla borde man i simulationer kunna skapa de planeter som Kepler har hittat. Det är detta vi har gjort i denna tes. Vi har skapat ett datorprogram som heter PAOPAP (*Pebble Accretion Onto Planetesimals And Planets*) vilket är en statistisk kod för att simulera planetformation med pebble accretion i ett cirkelsegment av skivan. Med denna kod tittar vi på hur stora planeter man kan bilda beroende på storleken på cirkelsegment och hur mycket massa som finns tillgängligt i gruskornen.

Contents

Chapter 1

Introduction

Of the NASA space telescope Kepler's results in 2013 (Batalha et al. 2013), 1108 new planetary candidates were unveiled. During 16 months of photometric observations, over $190,000$ stars were observed with 127,816 observed for the entire duration of observations. Of these results a large amount of the planetary candidates are of super-Earth size, that is terrestrial planets with a mass below $10M_{\oplus}$, and with short periods. Out of the 1108 new planetary candidates the planet radii, $R_{\rm p}$, distribution is: 202 with $R_{\rm p} < 1.25R_{\oplus}$, 422 with $1.25R_{\oplus} \leq R_{\rm p} < 2R_{\oplus}$, 426 with $2R_{\oplus} \leq R_{\rm p} < 6R_{\oplus}$, 40 with $6R_{\oplus} \leq R_{\rm p} < 15R_{\oplus}$, and 15 with $R_{\rm p} \geq 15R_{\oplus}$. Putting the results into perspective, 91% of the candidates are of smaller size than Neptune. So there exists a lot of planets between Earth and Neptune radii, yet none of the solar system bodies have this size. It appears, given the existing data, that planets are formed with these radii quite often and for a theory of planet formation to be valid, it should be able to account for them.

To give a background of planet formation means spanning quite a few years back. The earliest papers mentioned in a review by Lissauer (1993) go as far back as the 18th century with Kant (1755) and Laplace (1796). Then the argument was that the nearly circular and coplanar orbits of our Solar System planets is evidence suggesting planet formation taking place in a flattened disk around the central star.

During the next two-hundred years there has been a lot of development. Failed models have helped narrow down the picture and successful ones have been improved upon. At about two-hundred years later in 1969 is when Viktor Safronov came out with his planetesimal hypothesis (Safronov 1972). While some different theories of planet formation exist like gravitational instability (Boss 1997), Safronov's model is currently very much in favour. In it planet formation is a process with multiple steps. In the beginning, small microscopic grains collide and grow by sticking to one another. They then grow to much larger sizes and are known as pebbles at around mm to cm sizes. The next size step is planetesimals with no strict definition on size. But at around 100 km to 1000 km we begin to call the bodies planetary embryos or protoplanets. It has been generally thought that planetesimals grow by collisions to form planets in previous models (Kokubo & Ida

1998). This is generally a time-consuming process however and as found in Lambrechts & Johansen (2012) the growth to planets can be rapidly sped up with the inclusion of pebble accretion onto the planetesimals.

Chondrules are also necessary to mention. While the general nature of pebbles are aggregates, meaning they can be thought of as clumps, chondrules are spherical silicate objects usually slightly smaller than a mm. They have been heated up at some point, molten and solidified into their current shape found inside so-called chondrites, a type of meteorite. Chondrules are important to planet formation because they can be dated and found to belong to the early solar system and imply some sort of heating process that must have existed in the early solar system (Johansen et al. 2014).

In this thesis we simulate the formation of super-Earths in a code called PAOPAP (*Pebble Accretion Onto Planetesimals And Planets*) to see whether current models of planet formation by pebble accretion are able to account for their existence. A positive result would both strengthen the model of pebble accretion for planet formation and offer an explanation for the existence of super-Earths around so many stars.

There are several parameters that can affect planetesimal growth by accretion in our model and several parameters are also changed over the course of time due to accretion. Among the affected parameters are the eccentricity and inclination of the planetesimals. We investigate the result of changing: (1), The size of the annulus, Δr, that the accretion takes place in and (2), the relative mass of pebbles in the protoplanetary gas, f_{par}, to the mass of the gas, and briefly (3), the size of the pebbles. The result compared is the radius and, through a constant density, the mass.

The layout of the thesis is as follows: In chapter 2 we explain the background physics that play a part in pebble accretion theory starting with gas drag which then leads into drift in the protoplanetary disk. Next we explain pebble accretion in the Bondi and Hill regimes before moving into planetesimal accretion mechanics and oligarchic growth. In chapter 3 we give a brief explanation of the code used for the simulations and explain in detail how the code is evolved over time and how it includes planetesimal collisions. Chapter 4 presents the different sets of results regarding the effect of annulus width, mass fraction, and pebble size on the pebble accretion scenario as well as a demonstration of oligarchic growth. In chapter 5 we discuss the implications of the results, present our conclusions from it and suggest further studies that can be done with the model. There exists one appendix which explains some of the variables used in the work.

Chapter 2

Theory

2.1 Gas drag

The pebbles in the protoplanetary disk will couple to the gas surrounding them. This means that unless the gas and the pebble move at the same velocity the pebble will experience some sort of acceleration. In order to properly model the movements of pebbles, it is important to understand their physics.

Drag force

The acceleration that the pebbles experience due to coupling to the gas can be expressed, as in Weidenschilling (1977a),

$$\dot{\mathbf{v}} = -\frac{1}{\tau_{\mathrm{f}}}(\mathbf{v} - \mathbf{u}), \tag{2.1}$$

where $\mathbf{v}$ is the pebble's velocity and $\mathbf{u}$ the velocity of the surrounding gas. The friction time, τ_{f}, is derived in Weidenschilling (1977a), which contains all the physics regarding interactions between the particle and the gas flow. It can be divided into different regimes, the first of which is called the *Epstein drag regime*. This regime is active when the particle size is smaller than the mean free path, λ (formally $(9/4)\lambda$). The friction time in this regime is defined as

$$\tau_{\mathrm{f}} = \frac{R\rho_{\bullet}}{c_{\mathrm{s}}\rho_{\mathrm{g}}} \tag{2.2}$$

where R is the pebble radius, $\rho_{\bullet}$ is the material density, c_{s} the gas sound speed, and ρ_{g} the density of the gas.

The next regime, the *Stokes drag regime*, enters when pebbles are larger than 9/4 times the mean free path. Here, the friction time is expressed

$$\tau_{\mathrm{f}} = \frac{R\rho_{\bullet}}{c_{\mathrm{s}}\rho_{\mathrm{g}}}\frac{4}{9}\frac{R}{\lambda}. \tag{2.3}$$

In this regime the friction time is proportional to the squared radius but independent of the gas density as λ is inversely proportional to gas density.

The following transitions are not determined by the size of the particle but rather the *Reynolds number* defined as $Re = (2R\delta v)/\nu$ where ν is the kinematic viscosity, $\nu = (1/2)c_{\rm s}\lambda$, and $\delta v = |\mathbf{v} - \mathbf{u}|$ is the speed of the particle relative to the gas. The Reynolds number determines the transition to the next regimes which are non-linear. First when it equals unity, an intermediate regime is entered with $\tau_{\rm f} \propto (\delta v)^{-0.4}$. After $Re = 800$ the drag force becomes quadratic in relative velocity and the friction time can be defined

$$\tau_{\rm f} = \frac{6R\rho_\bullet}{(\delta v)\rho_{\rm g}}. \tag{2.4}$$

The transition between regimes is step-wise and occurs in the optically thin minimum mass solar nebula (abbreviated MMSN)(Hayashi 1981) with a power-law index of -1.5 for surface density (Weidenschilling 1977b) and 0.5 for temperature at the following list of particle sizes

$$R_1 = \frac{9\lambda}{4} = 3.2 \text{ cm} \left(\frac{r}{\rm AU}\right)^{2.75}, \tag{2.5}$$

$$R_2 = \frac{\nu}{2\delta v} = 6.6 \text{ cm} \left(\frac{r}{\rm AU}\right)^{2.5}, \tag{2.6}$$

$$R_3 = \frac{800\nu}{2\delta v} = 52.8 \text{ cm} \left(\frac{r}{\rm AU}\right)^{2.5}, \tag{2.7}$$

where Epstein to Stokes is R_1, Stokes to non-linear is R_2, and non-linear to quadratic is R_3.

It is necessary for us now to define the Stokes number from the friction time,

$$St = \Omega_{\rm K}\tau_{\rm f}, \tag{2.8}$$

which is a dimensionless parameter. Here $\Omega_{\rm K}$ is the Keplerian frequency at the given orbital distance. Since the inverse Keplerian frequency is a natural reference time-scale for a multitude of physical effects in the protoplanetary disk, the Stokes number determines several things. Some of these will be described in detail in later sections. They are, i) turbulent collision speeds, ii) sedimentation, iii) radial and azimuthal particle drift, iv) concentration in pressure bumps and vortices, and v) concentration by streaming instabilities. The Stokes number clearly is an important parameter for the physics used.

Radial & azimuthal drift

In the center of the protoplanetary disk is the central star. Due to dust build-up near the star, the density is increased and together with the heat from the star there is radial pressure support pointing outwards. So the gas in the protoplanetary disk experiences an outward pressure. With the gas pressure supported it moves around the star at a velocity below what is normally required for stable orbits. This is called a sub-Keplerian speed,

since Keplerian speed refers to the velocity needed without pressure support to remain at a certain orbit. The Keplerian speed is defined as

$$v_{\mathrm{K}} = \sqrt{\frac{GM}{r}} \tag{2.9}$$

where G is the gravitational constant, M is the mass of the star, and r is the distance from the star. We can write the difference between the sub-Keplerian gas velocity, v_{gas} and the Keplerian speed as

$$\Delta v = v_{\mathrm{K}} - v_{\mathrm{gas}}. \tag{2.10}$$

Another expression from Nakagawa et al. (1986) for this difference is

$$\Delta v = -\frac{1}{2}\left(\frac{H}{r}\right)^2 \frac{\partial \ln P}{\partial \ln r} v_{\mathrm{K}} \tag{2.11}$$

where P is pressure and H is the scale height. By looking at the forces at play we can find an expression for the gas velocity. The three forces involved are gravity, the pressure force, and the centripetal force.

$$F_{\mathrm{P}} + F_{\mathrm{c}} = F_{\mathrm{g}} \tag{2.12}$$

or

$$\frac{v_{\mathrm{gas}}^2}{r} = G\frac{M}{r^2} + \frac{1}{\rho}\frac{\partial P}{\partial r} \qquad \Longleftrightarrow \qquad v_{\mathrm{gas}}^2 = v_{\mathrm{K}}^2 + \frac{r}{\rho}\frac{\partial P}{\partial r} \tag{2.13}$$

which then gives the expression

$$v_{\mathrm{gas}} = \sqrt{v_{\mathrm{K}}^2 + \frac{r}{\rho}\frac{\partial P}{\partial r}}. \tag{2.14}$$

By expressing pressure as density times speed of sound squared, $P = c_{\mathrm{s}}^2 \rho$ and the equation for the scale height $H/r = c_{\mathrm{s}}/v_{\mathrm{K}}$ we find

$$v_{\mathrm{gas}} = \sqrt{1 + \frac{H^2}{r^2}\frac{r}{P}\frac{\partial P}{\partial r}}\, v_{\mathrm{K}}. \tag{2.15}$$

Expressed as the difference we get

$$\Delta v = v_{\mathrm{K}} - v_{\mathrm{gas}} = \left(1 - \sqrt{1 + \frac{H^2}{r^2}\frac{\partial \ln P}{\partial \ln r}}\right) v_{\mathrm{K}} \tag{2.16}$$

which gives equation 2.11 through a Taylor expansion. Equation 2.11 is roughly constant for the minimum mass solar nebula (Hayashi 1981) since $H/r \propto r^{1/4}$ and the pressure gradient in the midplane is $\partial \ln P / \partial \ln r = -3.25$. The value we get is $\Delta v \approx 50$ m/s.

Describing the drift speed of the particles in the gas in radial and azimuthal directions respectively we find, as shown by Weidenschilling (1977a) and Whipple (1972),

$$v_{\mathrm{r}} = -\frac{2\Delta v}{St + St^{-1}}, \tag{2.17}$$

$$v_{\phi} = v_{\mathrm{K}} - \frac{\Delta v}{1 + St^2}. \tag{2.18}$$

For the Epstein and Stokes regimes, these equations give the drift speed directly. The non-linear and quadratic regimes can be solved for with an iterative method. As in Lambrechts & Johansen (2012), these speeds can be combined to give the total relative velocity between a particle and a planetesimal in pure Keplerian rotation. It follows as

$$\Delta v_{\mathrm{rel}} = \frac{\sqrt{4St^2 + 1}}{St^2 + 1}\eta v_{\mathrm{K}}, \tag{2.19}$$

where η is a measure of the pressure support. Indeed, our original Δv is defined $\Delta v \equiv \eta v_{\mathrm{K}}$. For particles of appropriately small size equation 2.19 is well approximated by equation 2.11.

2.2 Pebble accretion

Now that we have discussed the motion of the pebbles in the gas we will go through the physics of their accretion onto the, comparatively, large planetesimals. We find that pebble accretion also takes place in different regimes.

We start off with *drift accretion*, or Bondi accretion, where we can define an outer radius from which particles moving at the speed Δv (where we now assume $\Delta v = \Delta v_{\mathrm{rel}}$) are significantly gravitationally deflected. We ignore stellar tidal field and Coriolis force here and arrive at the *Bondi* radius

$$R_{\mathrm{B}} = \frac{GM_{\mathrm{p}}}{\Delta v^2} \tag{2.20}$$

where M_{p} is the mass of the planetesimal. It is a valid approximation to ignore the stellar tidal field while the mass of the planetesimal is sufficiently small.

This is before the mass of the planetesimal has grown to a point where the Bondi radius is as large as the *Hill* radius. The drift regime then moves over into the Hill accretion regime. The Hill radius is the radius to the Hill sphere, which is the sphere of space where the gravity of the planetesimal dominates over the tidal forces from the central star. The mass at this transition can be written as

$$M_{\mathrm{t}} = \sqrt{\frac{1}{3}}\frac{\Delta v^3}{G\Omega_{\mathrm{K}}}. \tag{2.21}$$

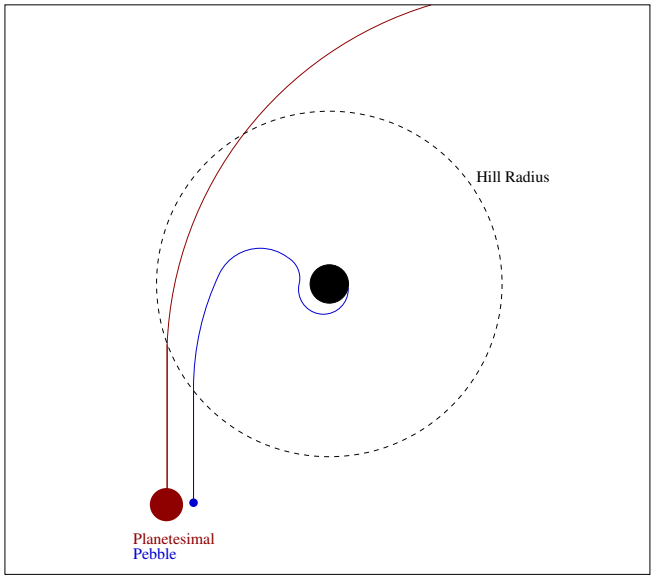

Figure 2.1: This figure shows the effect of coupling to the gas drag for passing particles of different sizes. The pebble (blue), coupled to the gas, is unable to escape accretion by the central planetesimal as expressed in equation 2.22. The planetesimal (brown) is too large to couple to the gas however and is gravitationally scattered instead.

This transition marks a boundary where the relative speed of the pebbles in the gas is first determined by the headwind of the gas (i.e Δv), and after the transition by the Hill speed which is defined through the equation $v_{\rm H} = \Omega_{\rm K} R_{\rm H}$.

Going back to drift accretion, whether or not a particle is accreted depends on the balance between gravitational attraction and the drag force. A particle can be pulled from the flow of the gas if enough energy is dissipated during deflection. If the time to cross the Bondi radius, $\tau_{\rm B} = R_{\rm B}/\Delta v$, is similar to the friction time, $\tau_{\rm f}$, the drag force will cause the particles to spiral inward from the Bondi radius. This leads to an effective accretion radius. If $\tau_{\rm B} > \tau_{\rm f}$ the pebbles are strongly coupled to the gas. Here, grazing particles, particles that are deflected on time-scales shorter than the friction time are pulled out of the flow. Denoting gravitational attraction by the acceleration g we can get the deflection time, t_g, and a criterion for accretion,

$$t_g = \frac{\Delta v}{g} < \tau_{\rm f}. \tag{2.22}$$

Since this deflection time is given by $(\Delta v) r^2/GM_{\rm p} = (r/r_{\rm B})^2 \tau_{\rm B}$ we are able to use the criterion in equation 2.22 to solve for an expression for the accretion radius. It becomes

$$\frac{R_{\rm acc}}{R_{\rm B}} = \left(\frac{\tau_{\rm B}}{\tau_{\rm f}}\right)^{-1/2}, \tag{2.23}$$

which is for strongly coupled particles.

We can now express the accretion rate in the drift accretion regime.

$$\dot{M}_{\rm d} = \pi \rho_{\rm p} R_{\rm acc}^2 \Delta v \tag{2.24}$$

where $\rho_{\rm p}$ is the pebble density. The expression is valid for when $R_{\rm acc}$ is smaller than the pebble scale height $H_{\rm p}$. When they become comparable the expression changes to

$$\dot{M}_{\rm d} = 2 R_{\rm acc} \Sigma_{\rm p} \Delta v, \tag{2.25}$$

where $\Sigma_{\rm p}$ is the pebble column density.

Next, we enter the Hill accretion regime mentioned earlier. The planetesimals mass grows until the Bondi radius, $R_{\rm B} \propto M_{\rm p}^2$, is comparable to its Hill radius, $R_{\rm H} \propto M_{\rm p}^{1/3}$. It then crosses the transition mass of equation 2.21. This brings about a change in the pebble accretion mechanism. Once $M_{\rm p} > M_{\rm t}$ the pebbles at the edge of the Hill sphere move towards the planetesimal with the relative velocity $v_{\rm H}$. As before with the drift accretion regime, only when the gravitational deflection time is comparable to the friction time will enough energy be dissipated during approach to ensure the accretion of the pebbles. But if it holds true, the pebbles accrete from the Hill sphere and we can express the accretion rate as

$$\dot{M}_{\rm H} = 2 R_{\rm H} \Sigma_{\rm p} v_{\rm H} \propto M_{\rm p}^{2/3} \tag{2.26}$$

2.3 Planetesimal accretion

The contribution of accreting planetesimals onto protoplanets is still a vital part of the planet formation stage even thought it takes much longer to form planets without the inclusion of pebble accretion. Both appear to carry an important role in planet formation and we will see later on how one compares to the other. Collisions between planetesimals operates under different physics from pebble accretion and gas drag.

Collisions and gravitational focusing

In the population of planetesimals collisions are an important part of the growth process. Still many use it as the dominant means of terrestrial planet formation (Armitage 2010). In Armitage's book, they review the physics of planetesimal collisions and we will briefly go over it here as it is still an integral part of the evolution of the terrestrial planets.

We consider two bodies approaching one another with relative velocities $\sigma/2$, masses m, and radius R. They move on a trajectory with an impact parameter b. Without gravitational focusing of the cross-section, they will only collide if $b < 2R$. That is to say their cross-section would be $\Gamma = 4\pi R^2$. Gravity however, will change the trajectories and the

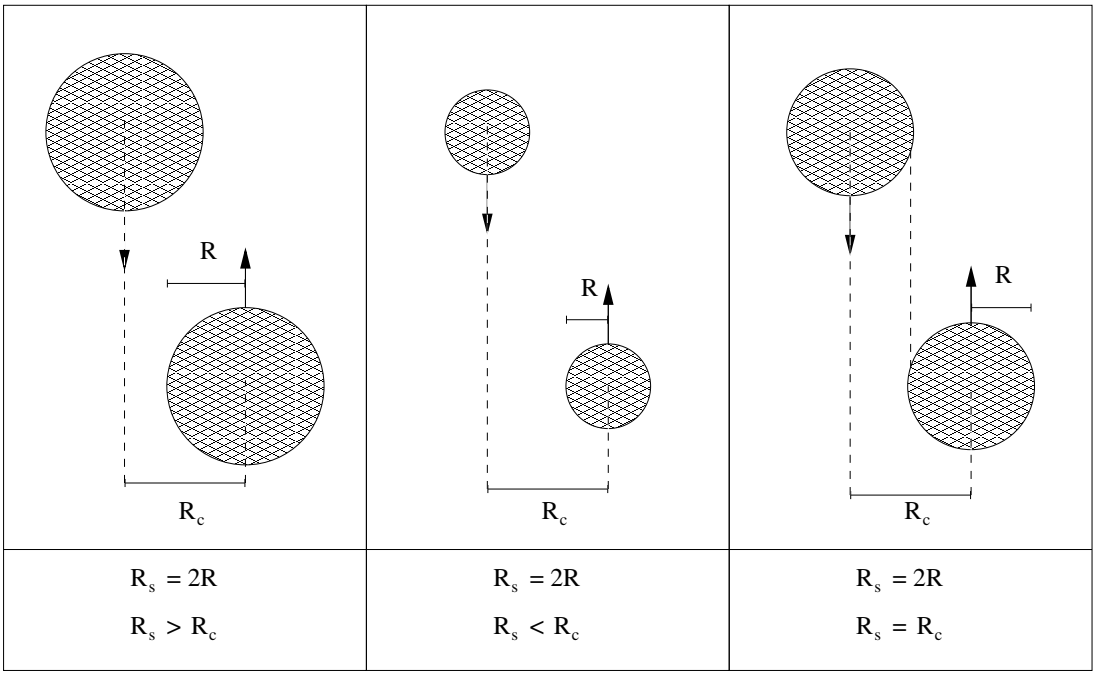

Figure 2.2: To illustrate the relationship between two bodies at closest separation with radius,R, closest separation, $R_{\rm c}$, and collisional outcome three situations are shown. Starting from the left the sum of the radii, $R_{\rm s}$, is larger than the closest approach. ($R_{\rm s} > R_{\rm c}$). This results in a collision as the bodies pass each other. In the middle, $R_{\rm s} < R_{\rm c}$ and a flyby will occur. In the right scenario, $R_{\rm s} = R_{\rm c}$ and a grazing collision will occur.

two bodies will move closer. The closest approach gives separation $R_{\rm c}$ and maximum velocity $v_{\rm max}$. Conservation of energy between infinite separation and closest approach thus gives

$$\frac{1}{4}m\sigma^2 = mv_{\rm max}^2 - \frac{Gm^2}{R_{\rm c}} \tag{2.27}$$

where the left side is the total kinetic energy at infinite separation and the right hand side gives kinetic energy and gravitational potential at closest approach. At closest approach there is no radial component of the velocity and together with angular momentum conservation we get

$$v_{\rm max} = \frac{1}{2}\frac{b}{R_{\rm c}}\sigma. \tag{2.28}$$

We note that the sum of the two radii is $R_{\rm s}$. This means that for $R_{\rm s} > R_{\rm c}$ a collision will occur and conversely for $R_{\rm s} < R_{\rm c}$ only a flyby will occur. Thus the largest value b for collision is

$$b^2 = R_{\rm s}^2 + \frac{4GmR_{\rm s}}{\sigma^2}. \tag{2.29}$$

By using the escape velocity at contact $v_{\rm esc}^2 = 4Gm/R_{\rm s}$ we can express equation 2.29 as

$$b^2 = R_{\rm s}^2 \left(1 + \frac{v_{\rm esc}^2}{\sigma^2}\right). \tag{2.30}$$

Thus the cross-section is enhanced by gravity to become

$$\Gamma = 4\pi R^2 = \pi R_{\rm s}^2 \left(1 + \frac{v_{\rm esc}^2}{\sigma^2}\right). \tag{2.31}$$

This immediately tells us that dynamically cold disks with smaller random velocities will have greater cross-sections and a greater rate of collisions.

Not all collisions contribute to growth however as too much energy during an impact can lead to dispersal which means that the colliding objects are shattered and do not re-accrete. Another possibility is fragmentation followed by re-accretion but this does not leave a solid body. The only outcome that generates growth is accretion. We define the specific energy (energy per unit mass) of the collision as

$$Q \equiv \frac{mv^2}{2M} \tag{2.32}$$

where an impactor with mass m hits mass M at speed v. It is this specific energy, Q, which largely decides what outcome will result from the collision. We can define some boundaries. $Q_{\rm D}^*$ as the minimum energy for dispersion into two or more pieces. $Q_{\rm S}^*$ as the minimum energy for shattering, fragmentation with re-accretion. Of course $Q_{\rm D}^* > Q_{\rm S}^*$. The former, $Q_{\rm D}^*$, has two regimes as well. The strength dominated regime where small bodies require large material strength to withstand impacts. In this regime $Q_{\rm D}^*$ decreases with size due to defects growing more commonplace. The other regime is the gravity dominated. In it large bodies are held together by gravity and $Q_{\rm D}^*$ must exceed the specific binding energy of the target. The binding energy is scaled with mass, M and radius, R, as

$$Q_{\rm B}^* \propto \frac{GM}{R}. \tag{2.33}$$

This is not a good estimate of $Q_{\rm D}^*$ but nevertheless $Q_{\rm D}^*$ increases with size.

In the code used, all collisions are treated as accretion scenarios however, meaning that specific energy is not of importance to the simulations. For large planetesimals (>100 km), it is well-known that they are strong enough to survive high-speed collisions (Bottke et al. 2005). Further motivation can be found in Johansen et al. (2015).

Oligarchic growth

From the work of Kokubo & Ida (1998) it has become evident that the stage of growth including protoplanets undergoes a separation into an oligarchy of a few larger bodies effectively isolated from one another, resulting in an eventual isolation mass. We can see this kind of behaviour in figure 2.3.

There are two stages of growth to consider with the first being runaway growth. It has been found that during early stages of accretion the larger planetesimals grow more rapidly, a behaviour we see in our results and which is due to the gravitational focusing derived earlier in this section. This results in runaway growth of the largest planetesimals. Interestingly however is that eventually, when entering the so-called post-runaway accretion stage, the largest planetesimals, having become protoplanets, experience a slowing down in growth when they become large enough to affect the local velocity dispersion of planetesimals.

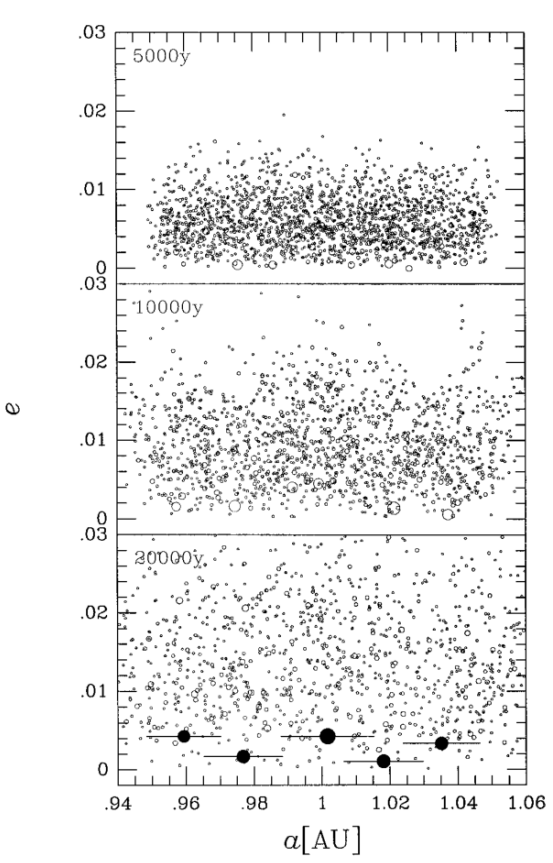

Figure 2.3: Figure 4 from Kokubo & Ida (1998) showing the growth into an oligarchy without any seed planetesimals.

In the protoplanet stage orbital repulsion comes into play as well. The protoplanets repel one another and expand their orbital separation if the separation is smaller than about $5R_{\mathrm{H}}$, where the Hill radius is given as

$$R_{\mathrm{H}} = \left(\frac{M_1 + M_2}{3M_\odot}\right)^{1/3} a, \qquad (2.34)$$

where M_1 and M_2 are the protoplanet masses and $M_\odot$ is the solar mass. a is the semi-major axis. Expansion of orbital separation is a coupling effect from scattering of large bodies and dynamical friction. If we have two protoplanets on circular orbits scattering against one another they will increase both eccentricity and separation. The eccentricity is returned to normal due to dynamical friction but the separation is not. Kokubo & Ida (1998) find a typical orbital separation of $10R_{\mathrm{H}}$.

When combining the growth with the orbital separation, the protoplanets will retain a $5R_{\mathrm{H}}$ during growth with separation scaled by the Hill radius. So orbital separation increases with mass and semi-major axis of the protoplanets. Between the two protoplanets the larger one grows more slowly, as is explained above. The growth of the protoplantets will still be faster than the planetesimals however and the end result is an oligarchic growth of the protoplanets as they sweep up the nearby planetesimals. It is also due to this oligarchic growth stage that planet formation is not faster since the moment they reach an isolation mass, growth stops. The large oligarchs slowly perturb one another's orbits so that they cross. The protoplanets then grow in giant impacts.

Chapter 3

Method

3.1 PAOPAP

The code we have used for simulating the growth of the planetesimals and planets is called PAOPAP - Pebble Accretion Onto Planetesimals and Planets. It was created for simulating chondrule accretion onto planetesimals in Johansen et al. (2015). It is a numerical code used to solve for the evolution of mass, eccentricity and inclination over time for a set of planetesimal bodies. While our results focus on the size evolution, we will explain the code in full.

PAOPAP operates with planetesimals as individual particles marked by their mass, eccentricity and inclination. The first is evolved through both pebble accretion onto the planetesimal but also planetesimal collisions. The two latter properties are affected through viscous stirring, dynamical friction of planetesimals and damping brought on by gas drag, pebble accretion and scattering.

In an effort to conserve time, the code separates the particles into discrete size bins before calculating the temporal evolutions mentioned but does so for the smallest and largest planetesimals in every bin. By doing this the evolution of the other planetesimals can be found through interpolation from the two anchors. There are 200 bins spaced logarithmically between 10 km and 10 000 km.

The density of the pebbles is brought in through a Gaussian stratification profile with scale-height, H_{p}, for each bin set according to the diffusion-sedimentation expression.

$$\frac{H_{\mathrm{p}}}{H_{\mathrm{g}}} = \sqrt{\frac{\alpha}{St + \alpha}}. \tag{3.1}$$

H_{g} is the scale-height for the gas, St the Stokes number again and α the turbulent viscosity. To better understand this equation we can look at the two limits of very small and very large St. If $St \ll \alpha$ the scale height of the pebbles is the same as that of the

surrounding gas. If on the other hand $St \gg \alpha$ the right side of the expression becomes $\sqrt{1/St}$ which means the pebbles have a much larger density than the gas. The friction time is familiar to us from the theory and varies depending on regime. We can get all the disk parameters necessary in the calculation of the particle scale height from the MMSN by setting a semi-major axis from the central star.

At the start of the simulation, a fraction of the mass of the gas, selected by us, is assigned to be pebbles. More pebbles are also created continuously over the first 3 million years of the simulation. The motivation for this is that chondrules have been found with ages varying between 0 to 3 million years.

The radii of the pebbles are set to be between 0.01 mm and 0.8 mm and they are divided into 30 different bins that are separated logarithmically. Their number density has a distribution of $\mathrm{d}n(a)/\mathrm{d}a \propto a^{-3.5}$. The planetesimals are initially distributed between sizes of 10 km and 150 km according to the distribution $\mathrm{d}N/\mathrm{d}R \propto R^{-2.8}$. It is however truncated using a super-exponential term $e^{-\left(\frac{R}{R_{\mathrm{exp}}}\right)^4}$ with $R_{\mathrm{exp}} = 100$ km. The total mass assigned to the planetesimal seeds is determined by the size of the annulus with 0.04 M_{E} for every 0.2 AU annulus width increase. The very small planetesimals will not show any significant growth and instead are useful for the dynamical friction they offer, which can reduce inclinations and eccentricities for other bodies of the simulation.

To get the pebble accretion rate for each planetesimal, interpolation in a look-up table is done to produce the accretion radius for a grid of values of planetesimal size normalised by Bondi radius, R/R_{B}, and friction time normalised by Bondi time, $\tau_{\mathrm{f}}/\tau_{\mathrm{B}}$. The look-up table is based on a large number of integrations of pebbles individual dynamics when passing a planetesimal with sub-Keplerian speed.

The column density of the gas is taken from the MMSN using a value of $\Sigma_g = 1700 g/cm^{-2}$. The MMSN is constructed with a rather easy-to-follow logic. By calculating the smallest amount of mass required in a disk to create the current solar system, Hayashi (1981) derived the first MMSN model. Understandably it depletes over time as the central star accretes mass and does this on an e-folding time-scale of 3 million years.

To handle oligarchic growth and the eventual isolation of a few large bodies that occur, the large oligarchic particles are identified as ones that can fit their combined reach of $10R_{\mathrm{H}}$ into the width of the modelled annulus. The bodies which are within this range are not allowed to accrete one another but as the planetesimals grow, there will not be room for all the previous oligarchs and the smallest ones will be pushed out and possibly accreted by one of the oligarchs. For the oligarchs, inclination perturbations and dynamical friction in eccentricity is ignored.

3.2 Euler's method

To get the temporal evolution our three parameters, that is $\dot{M}$, $\dot{e}$, and $\dot{i}$, we use a simple Eulerian scheme. While it is familiar to most, we will briefly go through the basics of the method here.

Assuming we have an initial value problem with $y' = f(t, y(t))$ and $y(t_0) = y_0$. Introducing a time-step, dt which can be variable or fixed, we move in time with a step from t_0 to $t_1 = t_0 + h$, or more generally $t_{n+1} = t_n + h$. We can then take a Eulerian step defined as

$$y_{n+1} = y_n + hf(t_n, y_n), \tag{3.2}$$

which puts into context the approximative nature of the Eulerian method as the above equation states that the value y_{n+1} is equal to the previous function value, plus a linear step with the derivative at the previous value. The Eulerian method is an approximative solution to ODEs.

In our simulation, the time-step is determined so that M, e, and i do not change by more than 10%.

It might be argued that a higher order integration scheme should be used for the code. While higher order schemes in general offer greater detail, the PAOPAP code is a statistical one and thus in a calculation either something transpires or does not. For that end a simple Euler scheme is precise enough. As a result, the code saves computational time by not having to calculate several derivatives. There would not be enough improvement in a higher order integration scheme to justify the extra computational time.

3.3 Planetesimal collisions

Since planetesimal collisions are an important part of the formation they are included in the code by a Monte Carlo method. The planetesimals are sorted into discrete size bins as before and calculated for each bin is average inclination and eccentricity. This is so that a collision rate matrix, r_{ij}, can be calculated for all combinations. The rates of collisions are calculated through a scheme described in the online supplement of Morbidelli et al. (2009).

The probability of collision, P_{ij}, between two planetesimals from bin i and j can be calculated from the time-step. If random number r is smaller than P_{ij} the planetesimals are collided and we assume perfect sticking, that is, accretion as described in the theory. The mass of the smaller of the two particles is added to the larger one and the small is removed from the simulation.

In Johansen et al. (2015) they performed several tests of the scheme to investigate its usability. The coagulation scheme was tested against an analytical equation with a constant kernel. They had excellent agreement with the analytical expression implying a correct implementation of the Monte Carlo collision scheme.

To test the collision rate calculation they tried to reproduce one of the plots from Morbidelli et al. (2009) which shows damping of e and i due to mutual inelastic collisions. Specifically the shape of the damping is used for comparison to determine the accuracy of the collision rate. This also shows excellent agreement and thus the collision rate algorithm is properly included in PAOPAP.

The last test performed was in regards to the cumulative size distribution of planetesimals and was in good agreement with Morbidelli et al. (2009) despite the fact that the comparison paper contained fragmentation and Johansen et al. (2015) did not. It shows that fragmentation is not an important factor for coagulation of large planetesimals.

Chapter 4

Results

With chapter 2's theory and 3's code, we are able to simulate the formation of planets with the input parameters of our choice. In total, two sets of simulations were performed at initial distance of 1 AU in both cases. The first set of simulations are focused on increasing the width of the annulus, d_{ann}, around 1 AU in an effort to widen the region of accretion and to bring in more material to be accreted onto the planets. The only parameter being altered between simulations is the width of the annulus and it is changed between 0.2 AU and 1 AU. The second set of simulations instead keep a constant and rather thin annulus of 0.2 AU but alter instead a parameter called f_{par} which determines the amount of mass that is given to the pebbles. In other words, it gives more pebbles to be accreted. Initially a few simulations were done around moderate values of f_{par} before much larger values were tested. We also perform a simulation with larger pebble sizes to determine its effect and lastly we look at planetesimal size distribution for one of the simulations.

4.1 Broadening the annulus

We have tried to broaden the annulus to include more pebbles and in doing so tried to create larger planets by the end of the simulations. Five simulations were run with $d_{\text{ann}} = [0.2, 0.4, 0.6, 0.8, 1.0]$ AU. The input parameters set by us exist in a separate file. For these simulations they are presented in table 4.1.

The result after 10 million years of accretion is presented in figure 4.1 where lack a pattern. No correlation appears between the width of the annulus and the final mass of the largest planetesimal. This is possibly related to the growth into oligarchs. Widening the annulus is not going to have the desired effect if the planets end up with an isolation mass and are unable to accrete further. Another explanation could be that a second largest planet has formed with very similar mass. To study the evolution further we also plot the growth of M_{max} against the time in years to gain a view of what transpires during the simulation. The results are presented in figure 4.2 in regular form as well as with a logarithmic scale for the mass to see if there are any major changes during the early stages of evolution.

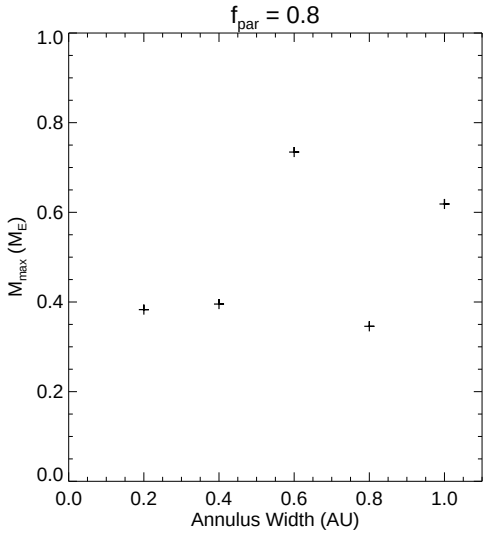

Figure 4.1: This figure shows the end results of the first set of simulations where the width of the annulus was increased. The mass of the largest planetesimal at the end of the simulation is plotted against the annulus width as crosses. Looking for any sort of structure we find none. An annulus width of 0.8 AU creates the smallest of all the planets we see in the plot. This is either a result of oligarchic growth giving the planets an isolation mass or because there are multiple planets around similar mass by the end of the simulation.

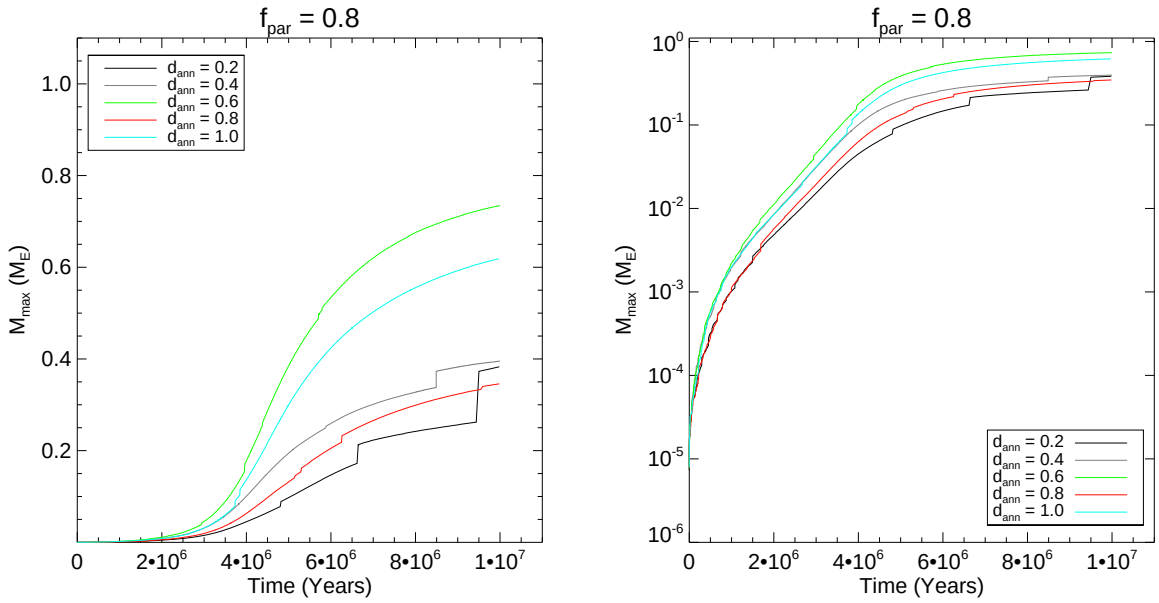

Figure 4.2: The temporal evolution of the mass of the largest planetesimal in the different d_{ann} simulations seen in a regular plot on the left and with a logarithmic y-axis on the right. Each simulation is colour-coded as in the legend. We can see how the end result can be determined by single late events as with $d_{\text{ann}} = 0.2$ which would likely be the smallest end mass if not for the giant collision at the end of its simulation.

The plots show us that the evolution of the 1.0 AU and 0.6 AU annulus transpire almost entirely through pebble accretion as there are no rapid jumps from planetesimal collision as seen very visibly in the 0.2 AU simulation. Despite a widened annulus there is no increase in the mass and the logarithmic plot proves that there are no surprising early events either and only some small collisions transpiring.

Table 4.1: The input parameters used for the simulations with varying annulus width. The name of the parameter is given along with its value and a brief description of it. The same input parameters are used for the simulations with f_{par} but then `rorb1` and `rorb2` are fixed instead as 0.2 AU.

Parameter	Value	Description
`rorb1`	Varied	Inner annulus radius
`rorb2`	Varied	Outer annulus radius
`nr`	1	Number of annuli
`fgas`	1.0	Fraction of MMSN mass in gas
`fpar`	0.8	Fraction of 1% of f_{gas}
`fmat`	0.5	Fraction of f_{par} created over time
`fpla`	0.1	Fraction of f_{par} in planetesimals
`cool`	1.0	Temperature relative to the MMSN
`apmin`	0.001 cm	Minimum pebble size
`apmax`	0.08 cm	Maximum pebble size
`qpeb`	3.5	Exponent in number density of pebbles
`tau_mat`	$1.5 \cdot 10^6$	e-folding timescale of dust turning into pebbles
`tau_acc`	$3 \cdot 10^6$	e-folding time-scale of gas accretion
`deltat`	$1.0 \cdot 10^{-4}$	Turbulent diffusion coefficient
`gammat`	$6.0 \cdot 10^{-5}$	Viscous stirring parameter
`Rmin`	10.0 km	Minimum size of initial planetesimals
`Rmax`	150.0 km	Maximum size of initial planetesimals
`Rexp`	100 km	Size at which planetesimal distribution is truncated
`gexp`	4.0	Power of super-exponential term when truncating
`qast`	2.8	Exponent in planetesimal size distribution
`rhomat`	3.5 g/cm^3	Material density
`vecc0`	$10.0 \cdot 10^2$ cm/s	Velocity relative to the circular orbit $v_{\mathrm{ecc}}^0 = e \cdot v_{\mathrm{K}}$
`tmax`	$1.0 \cdot 10^7$ years	Total length of simulations
`cdt`	0.1	Constant in determining the time-step
`dtsnap`	$1.0 \cdot 10^6$ years	Frequency of snapshots taken during simulation

4.2 Increasing f_{par}

To remind ourselves, f_{par} is the parameter that determines the amount of mass given to the pebbles in the simulation. It is defined in such a way that it is the fraction of a single

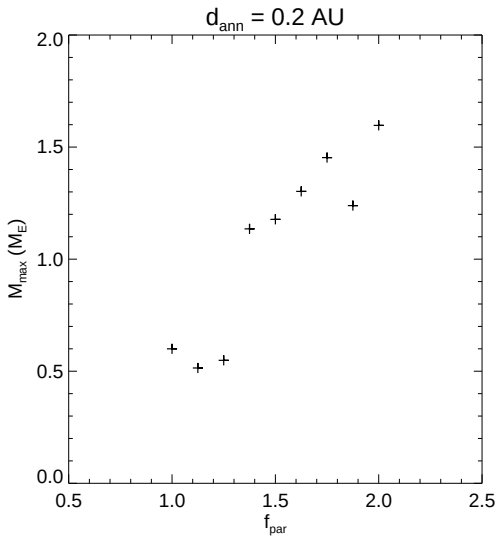

Figure 4.3: The end result of the first round of simulations in the second set where the fraction of pebbles was increased. The mass of the largest planetesimal at the end of the simulation is plotted against f_{par}. We see the beginning of a rather clear linear pattern emerging. Mass seems to increase with f_{par} in the results. There are no planets between roughly 0.5 and 1 Earth masses either due to multiple planets forming as seen in figure 4.4.

percent of another parameter f_{gas} which is given in mass to the pebbles. The parameter f_{gas} itself is a fraction of the MMSN that is given in mass to the gas. So if for example $f_{\mathrm{par}} = 10$, 0.1 of mass given to the gas in the simulation is instead given to the pebbles. For all of our simulations, f_{gas} has been set to unity, meaning we have assumed that the MMSN mass is present in our simulations. In the second set of simulations, we will split the presentation of results into two parts. This is because there were two rounds of the same type of simulations performed. Initially with a few closely spaced small values of f_{par} to compare results to the previous set of simulations and then afterwards with much larger values which incorporates the former.

Small values of f_{par}

Since the previous simulations had a constant value of $f_{\mathrm{par}} = 0.8$ we decided to investigate the effect a constant annulus width of 0.2 AU and changing the amount of pebbles within the annulus instead. The same input parameters as 4.1 were used with $r_{\mathrm{orb},1} = 0.9$ AU and $r_{\mathrm{orb},2} = 1.1$ AU and f_{par} varied instead between 1 and 2 with a step of 0.125 between simulations giving a total of 9 simulations. The end result of M_{max} is seen in figure 4.3 where one sees the beginning of a small linear correlation. Because of the small overall range in f_{par} it is hard to deduce large-scale correlation. There is a large gap between the three earliest simulations and the rest with no masses appearing between $\sim 0.5 M_{\mathrm{E}}$ and $\sim 1 M_{\mathrm{E}}$. To explain this, we extract the 10 largest bodies from the two f_{par} simulations,

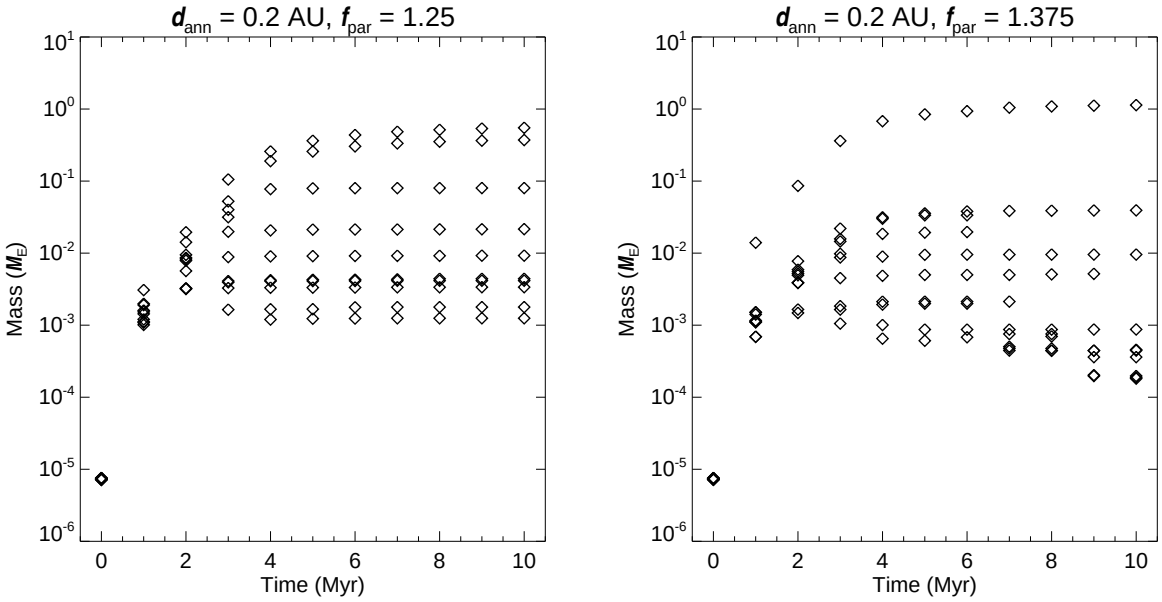

Figure 4.4: Ten largest planetesimals for $f_{\mathrm{par}} = 1.25$ and 1.375. The reason for the gap in figure 4.3 is seen as the left figure has a planet of almost the same mass in its simulation. In the right figure, a majority of the mass is kept in the largest planet.

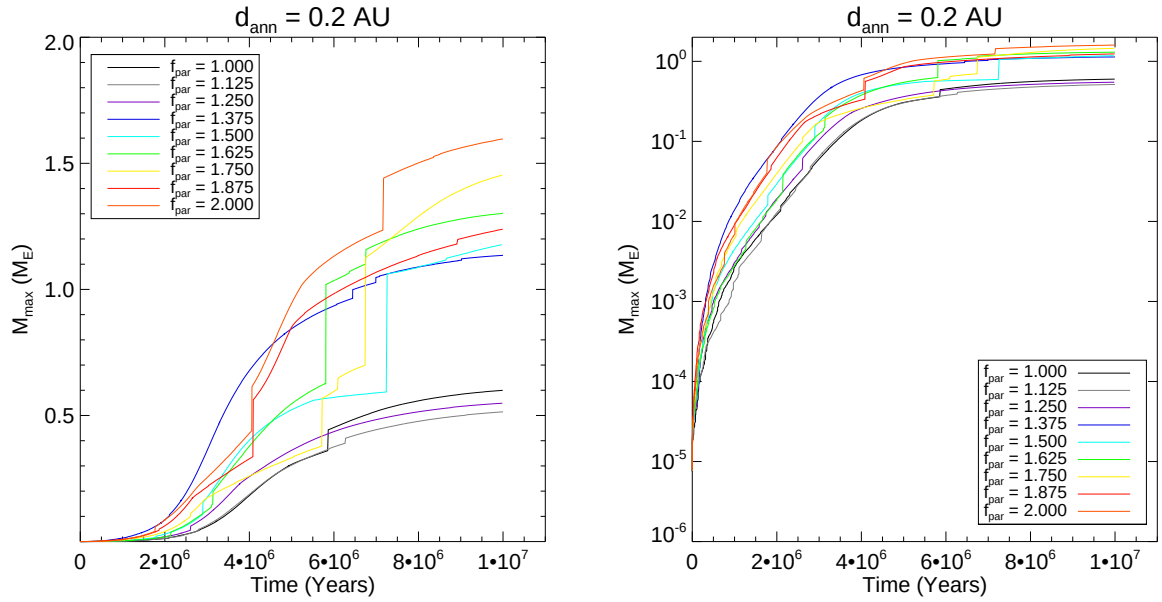

Figure 4.5: The temporal evolution of the mass of the largest planetesimal in the different small f_{par} simulations seen in a regular plot on the left and with a logarithmic y-axis on the right. We see the importance of giant impacts on these small planets. Some double their size due to giant impacts. Overall we are unable to grow planets larger than around 1.5 M_{E}. The right figure shows that there are no major jumps in mass very early on either.

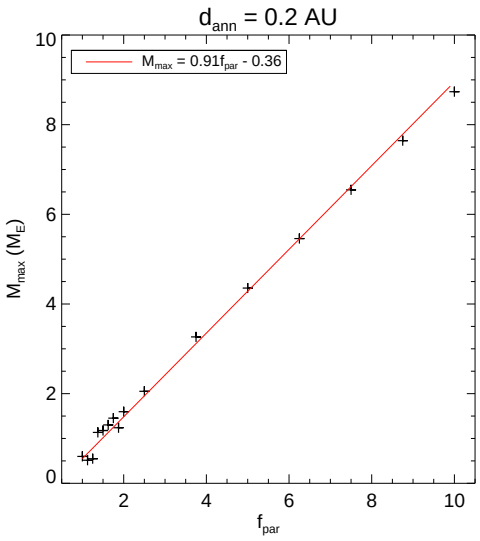

Figure 4.6: The mass of the largest planet plotted against the corresponding value of f_{par} in that simulation. A line is fitted (red) using linear regression along with the equation 4.1 to show the now very apparent correlation between mass and f_{par}. So while it is true that there is a correlation between large values of the parameter and the mass it is possible the behaviour at small values is non-linear. But super-Earth masses are attainable where the correlation is valid.

1.25 and 1.375 and plot them at every million years. The result we find is presented in figure 4.4. Here we find the explanation for the gap in figure 4.3 as the $f_{\mathrm{par}} = 1.25$ simulation has a planet of almost the same mass as the largest one. Since we extract the largest body in figure 4.3, this second body is hidden from us. We see in the $f_{\mathrm{par}} = 1.375$ simulation how no planets have similar mass as the largest one, explaining why it appears in figure 4.3 with a much larger mass.

Here as well we investigate the temporal evolution of all of the simulations to study the growth in full detail. The results can be seen in figure 4.5. We see quite clearly how important planetesimal collisions and giant impacts are for the final size of the planets as, for example, the $f_{\mathrm{par}} = 1.5$ simulation almost doubles in mass with a collision.

The simulations show the ability for pebble accretion to create Earth mass type planets. But since we are interested in creating the super-Earths of Kepler's data more massive planets are desired.

Large values of f_{par}

So to create even bigger planets we have used larger values of f_{par} ranging from 2.5 up to 10, stepping with 1.25 for each new simulation. The input parameters are the same as for the simulations with small f_{par}. To allow for easier comparison between the small and

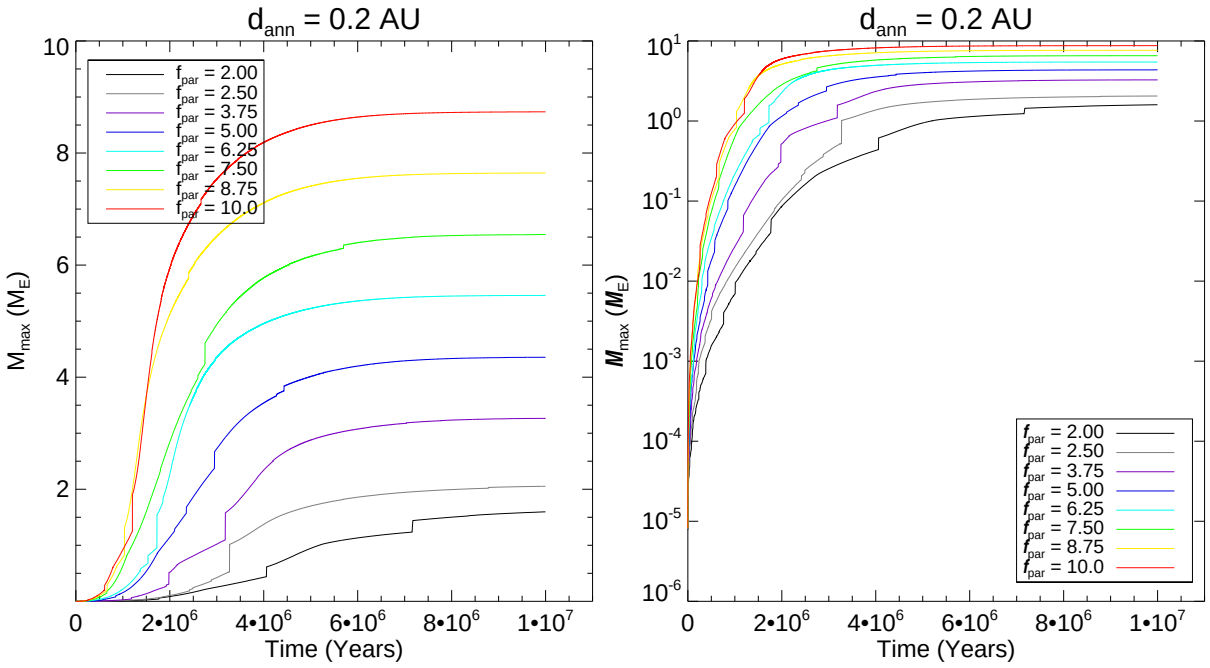

Figure 4.7: The temporal evolution of the mass of the largest planetesimal in the different large f_{par} simulations seen in a regular plot on the left and with a logarithmic y-axis on the right. We can see quite clearly here how the increasing f_{par}, with equidistant stepping produces planets with equidistant separation on the y-axis as well. We also see very clearly how ten million years is quite enough to produce the final mass of the planets in the simulations.

large f_{par} simulations we include the $f_{\mathrm{par}} = 2$ results from figure 4.5 in figure 4.7 and all the points from figure 4.3 in figure 4.6.

We begin by looking at the results in figure 4.6. When comparing to figure 4.3 we can see a much more evident linear correlation between the end masses. We have made a linear regression to fit a line onto the data points. The linear equation we find between M_{max} and f_{par} is

$$M_{\mathrm{max}} = 0.91 f_{\mathrm{par}} - 0.36. \tag{4.1}$$

While the linear behaviour does not appear at values below $f_{\mathrm{par}} = 2$, it is clear for larger values.

The temporal evolution is found in figure 4.7 where the correlation previously spotted in figure 4.6 is once more evident in the non-logarithmic figure. What we do see for large values of f_{par} is that the role of planetesimal collisions becomes restricted to earlier on. With the increased amount of pebbles available for accretion, the growth is much quicker for the largest planetesimal and it appears to accrete all nearby large planetesimals very early on (except for the oligarchs). Despite the increased mass, all simulations appear to

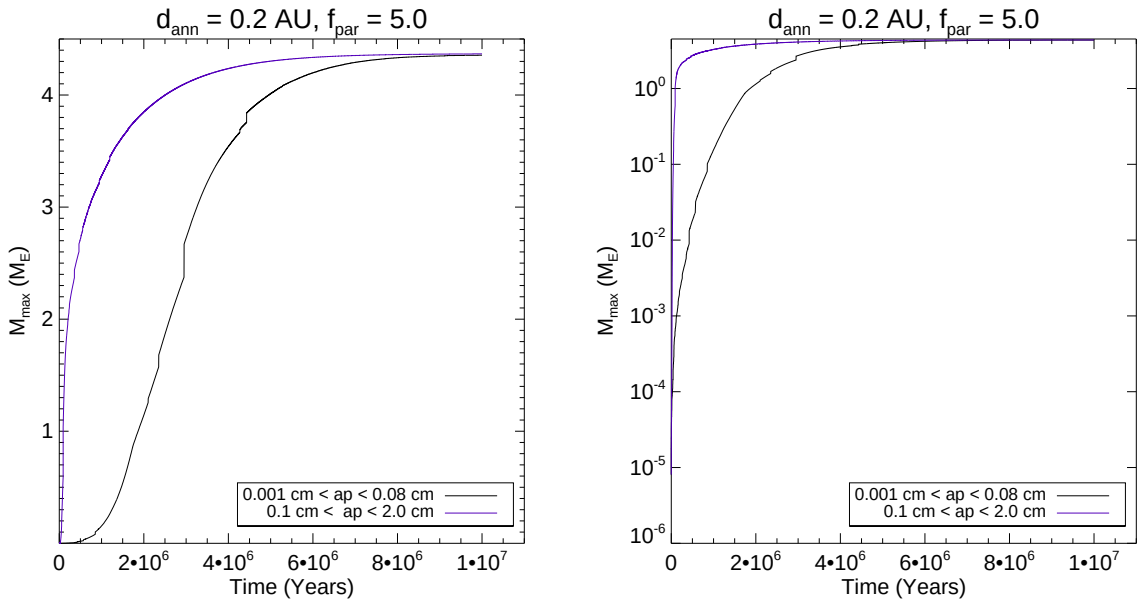

Figure 4.8: Temporal evolution of two simulations using $f_{\text{par}} = 5$ but differing in pebble sizes. Small pebbles (0.001 cm to 0.08 cm) are given in black and large ones (0.1 cm to 2.0 cm) are given in purple. Very little changes between the two simulations and the only visible change is the time it takes to reach the final mass. Larger pebbles causes the planetesimal to grow much faster in the beginning of the simulation but is eventually caught up to by the small pebble simulation.

reach their final mass at roughly 7 million years in, suggesting perhaps that the pebble accretion rate grows linearly with the amount of available pebbles.

4.3 Pebble sizes

While the usual and somewhat broad definition of pebbles is mm-cm, the values of ap_{min} and ap_{max} in table 4.1, used in every simulation, is set to strictly mm sizes, being 0.01 to 0.8 mm respectively. This is to correspond to typical sizes of chondrules which are small spherical droplets of glass found in chondrites. They are believed to contain traces of the building blocks of the planets in our solar system (Johansen et al. 2014) and it is for the purpose of simulating accretion of chondrules that PAOPAP was written. However chondrules can be classified as pebbles and there is no material difference in the simulations we have performed between a pebble and a chondrule. They are of the same material but different sizes.

But in order to determine whether or not it was an error to retain chondrule sizes for the pebbles we performed the $f_{\text{par}} = 5$ simulation from figure 4.7 but with $ap_{\text{min}} = 0.1$ cm and $ap_{\text{max}} = 2$ cm. The result of the simulation can be seen in figure 4.8.

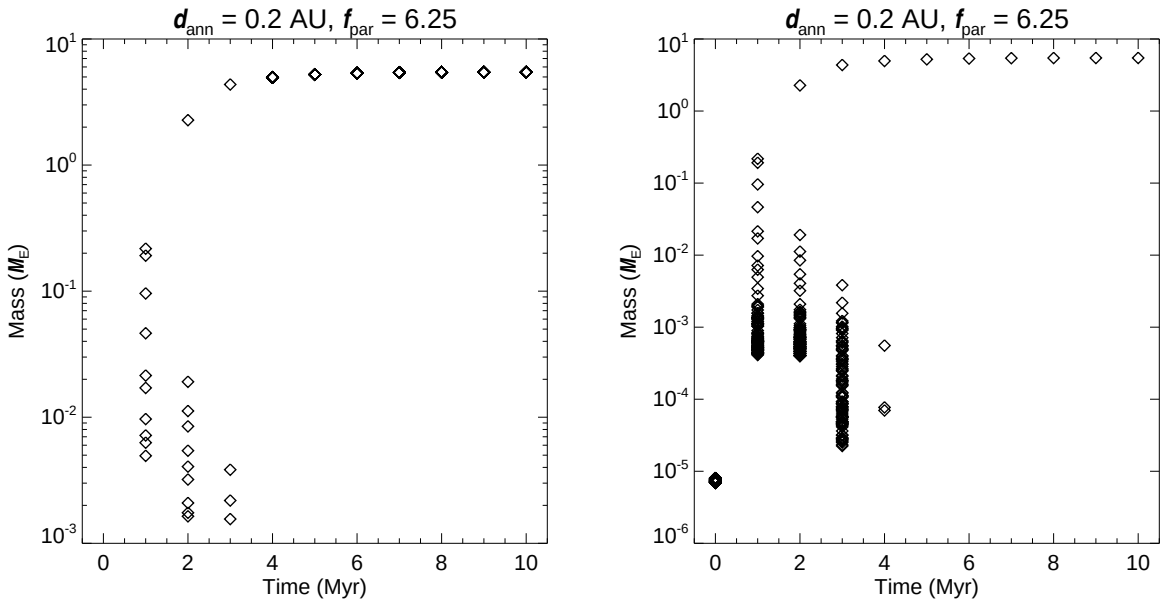

Figure 4.9: The size distributions of the (left) 10 largest planetesimals and (right) 100 largest using the $f_{\mathrm{par}} = 6.25$ simulation. The code handles the oligarchs by keeping the ones able to fit $10R_{\mathrm{H}}$ of their size within the modelled annulus. They are sorted in size as well. We can see that as one of the planets grows to large enough size, it becomes the only oligarch left to fit $10R_{\mathrm{H}}$ within 0.2 AU. The start of the simulation, $t = 0$ yrs, has yet to grow oligarchs and can only be seen in the right figure.

We see that the end mass ends up being almost the same for the largest planet. Instead, the main difference to note is how the simulation with larger pebbles grows with incredible speed at the beginning of the simulation and thus does not show any large number of planetesimal collisions as none of the other planetesimals are likely to become large enough to have a visible impact on the largest oligarch. By the time that the planetesimal in the small pebble simulation has reached $1M_{\mathrm{E}}$ the large pebble simulation planetesimal has reached a size almost four times as large. When looking at the logarithmic plot it is even more evident how much faster accretion takes place as the large pebble curve lies along the borders of the graph.

Since there is no real difference in the end mass though, we would only alter the size of the pebbles if we wished to reduce the time it takes to form the planets. The benefit of having used smaller pebbles in our simulations is that we see greater detail.

4.4 Planetesimal size distribution

We decided to investigate the evolution of not just the most massive planetesimal but of the oligarchs in one of the simulations. As is described in section 3.1, the code handles the oligarchs by taking the planetesimals in order of size tries to fit $10R_{\mathrm{H}}$ per planetesimal into the modelled annulus. The ones that fit inside are labelled oligarchs and are not allowed to accrete one another and only interact gravitationally.

To model these planetesimals, we extract the 10 and 100 largest planetesimals in two different plots. The simulation chosen for these plots is the $f_{\mathrm{par}} = 6.25$ simulation from the second set of simulations. The two results are found in figure 4.9. We can see that it matters very little whether we include 100 or 10 planetesimals as the majority of them simply clump together around very similar mass at the bottom. Initially all the planetesimals are located at below 10^{-5} M_{E} because growth has yet to start. We quickly see how pebble accretion creates a group of oligarchs and already at 2 Myrs into the simulation a very clear oligarch is created. By 4 Myrs, only three other planetesimals remain even when we sample the 100 largest. This means that only these planetesimals remain in our simulation. To understand this result and where the other planetesimals have gone we perform a quick calculation. At 4 Myrs the planet has a mass of about 5 M_{E} which corresponds to a Hill radius at 1 AU of roughly 0.012 AU. Then $10R_{\mathrm{H}} = 0.12$ AU. Since the modelled annulus is 0.2 AU there is not a lot of room left to fit their $10R_{\mathrm{H}}$ into the 0.2 AU distance. (Note that this is still however just a device for labelling oligarchs and that the bodies are not lined up dimensionally next to each other in the simulations). Only a few other small bodies remain and even later at 5 Myrs and forwards, only the largest body remains. So we can see how, towards the end of the simulation, the main body has become so large that it allows for no other oligarchs to exist and it can potentially accrete any other body.

Chapter 5

Conclusions

5.1 Isolation mass in increasing annulus width

One of the initial ideas was to somehow increase the amount of mass that could be accumulated by the planetesimals in the simulation and one of the two ways of doing this that we thought of was to try and increase the width of the annulus. The results found in figures 4.1 and 4.2 show us that there is no correlation when increasing the annulus as all that will occur is that either the dominating planetesimal will sweep up what it can before creating an empty annulus within our existing one, isolating itself, or we hide multiple planet systems by extracting only the largest planet as was seen in figure 4.4. Or perhaps both are present at the same time. Our planets never reached as far as one Earth mass. Since we are interested in the formation of super-Earths another means of growing large planets is required.

5.2 Growth with more pebbles

The most promising result for our purpose comes from simply increasing the amount of mass dedicated to the pebbles through the parameter f_{par}. We have successfully grown planets with masses up to 8 M_{E} or $1.6R_{\mathrm{E}}$ with Earth having its mean density of 5.514 g/cm^3. An Earth in our density of 3.5 g/cm^3 would mean we have formed up to 2 R_{E} planets. The results from Kepler (Batalha et al. 2013) have shown a large fraction of super-Earths within this size range which is very promising for our results. In the statistical code of PAOPAP we have successfully created super-Earths reminiscent of Kepler's results. Pebble accretion is capable of reproducing some of the observations.

Another result to highlight from the second set of simulations is the correlation between increasing f_{par} and the final mass. While initially large-scale correlation was not visible, the results found for oligarchic growth in figure 4.9 show us that only one large planetesimal or planet remains at the end of the simulation. If that is the case, then adding more mass into the system means it will be accreted onto this body and the mass added should correspond

to the mass gained by the planet. Similar understand was used to explain the dispersion in the largest mass found in the small f_{par} simulations in figure 4.3, as the pebble mass is sometimes spread across several oligarchs rather than just the one.

Our Kepler-sized planets are most likely all formed as single-planet systems. Figure 8 of Batalha et al. (2013) shows us that many of Kepler's super-Earths are in multiple planet systems. So in this regard, the results look less like Kepler's results.

5.3 Future work

Work that is left to be continued would be further simulations, perhaps with increased values of f_{par} as well as with different annuli. If oligarchs were handled in some different way PAOPAP might be used quite well for simulating the growth of even larger planets.

One of the things that the PAOPAP code does not do is to account for migration of the planetesimals. In the disk, planets are capable of migration (Raymond et al. 2006) both outwards and inwards. We initially created all of our planets at an annulus that was centered around 1 AU. This is much further out than most of Kepler's exoplanets. Some of the longest periods of Kepler's exoplanets were around 180 days while the majority were concentrated at around 10 day orbits. Because of this, we have assumed that our planets migrate inwards as this is certainly a possibility. To include migration and semi-major axis into the simulations would produce interesting results to see whether or not the produced planets look at all like the Kepler results. Including migration could explain the current presence of Kepler super-Earths in such tight orbits.

Bibliography

Armitage, P. J. 2010, Astrophysics of planet formation. (Cambridge, UK ; New York : Cambridge University Press, 2010)

Batalha, N. M., Rowe, J. F., Bryson, S. T., et al. 2013, The Astrophysical Journal Supplement Series, 204, 24

Boss, A. P. 1997, Science, 276, 1836

Bottke, W. F., Durda, D. D., Nesvornỳ, D., et al. 2005, Icarus, 175, 111

Hayashi, C. 1981, Progress of Theoretical Physics Supplement, 70, 35

Johansen, A., Blum, J., Tanaka, H., et al. 2014, Protostars and Planets VI, 547

Johansen, A., Mac Low, M.-M., Lacerda, P., & Bizzarro, M. 2015, Science Advances, 1, e1500109

Kant, I. 1755, Kant's Cosmology. New York: Greenwood

Kokubo, E. & Ida, S. 1998, Icarus, 131, 171

Lambrechts, M. & Johansen, A. 2012, A&A, 544, A32

Lambrechts, M. & Johansen, A. 2014, A&A, 572, A107

Laplace, P. 1796, Exposition du Système du Monde, Paris. English translation, HH Harte (1830) The System of the World

Lissauer, J. J. 1993, Annual review of astronomy and astrophysics, 31, 129

Lissauer, J. J., Ragozzine, D., Fabrycky, D. C., et al. 2011, The Astrophysical Journal Supplement Series, 197, 8

Morbidelli, A., Bottke, W. F., Nesvorný, D., & Levison, H. F. 2009, Icarus, 204, 558

Nakagawa, Y., Sekiya, M., & Hayashi, C. 1986, Icarus, 67, 375

Raymond, S. N., Mandell, A. M., & Sigurdsson, S. 2006, Science, 313, 1413

Safronov, V. S. 1972, Evolution of the protoplanetary cloud and formation of the earth and planets.

Weidenschilling, S. 1977a, Monthly Notices of the Royal Astronomical Society, 180, 57

Weidenschilling, S. 1977b, Astrophysics and Space Science, 51, 153

Weiss, L. M. & Marcy, G. W. 2014, The Astrophysical Journal Letters, 783, L6

Whipple, F. 1972, ed. A. Elvius, Wiley, London, 211

Appendix A

Variables

This appendix gives a list of variables used in the thesis with a description in a sentence or two. For the input parameters and their description, see table 4.1.

Table A.1: A list of variables used in the thesis.

Variable	Description
Δr or d_{ann}	The size of the annulus.
τ_{f}	Friction time. The timescale on which the drag force operates.
$\rho_{\bullet}$	The material density.
ρ_{g}	The volume density of the gas.
c_{s}	Speed of sound in the gas.
λ	The mean free path.
Re	The Reynolds number. It is the ratio of intertial forces to viscous forces.
δv	Relative speed of particle and gas.
ν	Kinematic viscosity.
St	The Stokes number. Definition in equation (2.8).
Ω_{K}	The Keplerian frequency.
v_{K}	Keplerian speed.
v_{gas}	Speed of gas.
H	Scale height.
F_{P}	The pressure force.
F_{c}	The centripetal force.
F_{P}	Gravitational force.
v_{r}	Radial drift speed of particle in gas.
v_{ϕ}	Azimuthal drift speed of particle in gas.
Δv_{rel}	Relative velocity between a particle and a planetesimal in pure Keplerian rotation.
R_{B}	Bondi radius, radius where particle are significantly deflected from a larger body.

Table A.2: Contd: list of variables used in the thesis.

Variable	Description
M_{t}	The mass at which Bondi/drift-accretion transitions to Hill accretion.
v_{H}	The hill velocity.
τ_{B}	The Bondi time. The time to cross the Bondi radius.
t_{g}	Time-scale for deflection.
g	Gravitational acceleration.
R_{acc}	The effective accretion radius.
$\dot{M}_{\mathrm{d}}$	Accretion rate in drift accretion.
ρ_{p}	The pebble density.
Σ_{p}	Surface density of the pebbles.
R_{H}	The Hill radius. Radius of the Hill sphere.
σ	Random velocity of planetesimals.
b	Impact parameter.
Γ	Cross-section.
R_{c}	Closest approach separation during gravitational focusing.
v_{max}	Velocity during closest approach.
R_{s}	Sum of approaching bodies radii.
v_{esc}	The escape speed. Speed required to escape gravity.
Q	Specific energy of a collision. Energy per mass.
Q^*_{D}	Minimum energy for dispersion into two or more pieces..
Q^*_{S}	Minimum energy for shattering, fragmentation and re-accretion.
Q^*_{B}	The binding energy of the target in collision.
α	Turbulent viscosity.
Σ_{g}	Gas surface density.
r_{ij}	Collision rate matrix.
P_{ij}	Probability of collision.
M_{max}	Largest mass in simulations.